



A NEW COMPACT FSIW FED DIELECTRIC RESONATOR ANTENNA FOR MILLIMETER WAVE BAND APPLICATIONS

Saeed FAKHTE¹, Ladislau MATEKOVITS^{2,3,4}

¹School of Electrical and Computer Engineering, Qom University of Technology, Qom, Iran

¹fakhte@qut.ac.ir

²Department of Electronics and Telecommunications, Politecnico di Torino, 10129 Torino, Italy

³Instituto di Elettronica e di Ingegneria dell'Informazione e delle Telecomunicazioni, National Research Council of Italy, 10129 Turin, Italy

⁴Department of Electronics and Telecommunications, Politehnica University Timisoara, Romania

²ladislau.matekovits@polito.it

Abstract

A new waveguide feeding scheme of a rectangular DRA based upon the folded substrate integrated waveguide concept is presented. The most important characteristics of this antenna are a good radiation efficiency of above 87% at high frequencies which antenna operates and half transverse size of its feeding in comparison with other waveguide feeding schemes such as SIW and rectangular waveguide. The simulated results show an impedance bandwidth of 6.7% from 25.25 to 27 GHz and a good gain of at least 5 dB for this range.

Key words: Dielectric Resonator Antenna, Folded Substrate Integrated Waveguide, Millimeter-wave band, radiation efficiency

1. Introduction

Dielectric resonators are widely used as microwave components in many applications such as oscillator and filter. Since advent of first paper investigating DR as an antenna [1], many researches have been devoted to this type of antenna [2-9]. Dielectric resonator antenna (DRA) was reported as a good candidate for low gain antennas such as dipoles and microstrip antennas [10-12]. The advantages of DRA compared to these antennas are design flexibility, lack of surface waves in structure, minimal conductor loss and wide impedance bandwidth [13]. Rectangular DRA often is used because of its fabrication simplicity and more degree of freedom

compared to other basic shapes such as cylindrical and hemispherical [14].

Since the advent of DRA many approaches for feeding the DRA have been proposed that includes microstrip line, coplanar waveguide, rectangular waveguide and recently aperture feeding through slot on wall of SIW [14,15]. By increase in operation frequency the radiation and conductor losses are considerably increased for microstrip line and coplanar waveguide. But instead, the SIW is a good candidate for high frequencies specially at millimeter wave band because of its closed form structure that reduces radiation loss [16]. The most important drawback of the SIW is its wide transverse size. For solving this problem some

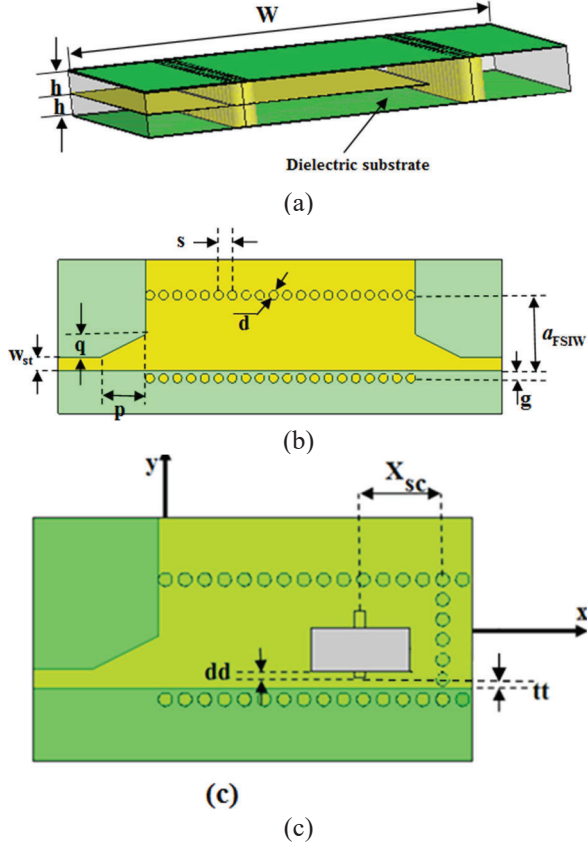


Fig. 1: (a) The geometry of a 2 port FSIW with transition to strip line (a) 3D view and (b) top view (c) the RDRA fed by the FSIW

new structure such as FSIW and HMSIW is proposed. These two structures have nearly half transverse size of the SIW ones but the same propagation constant and interior field distributions of that are noticed [17,18]. The FSIW and SIW have almost the same attenuation constants. But the attenuation constant of the HMSIW is high because of its high radiation loss in frequency band near the cutoff frequency. In fact, it is found that if the width of the FSIW is nearly the half of the width of the original SIW and its height is twice that of the SIW, the FSIW has nearly the same propagation and cutoff characteristics as the SIW [18].

However, in this work for the first time the FSIW feeding scheme is presented for exciting the DR. Low radiation loss and miniaturized structure are the most important features of the proposed combination. This paper is organized as follows. In Section 2 design guidelines are presented and the FSIW design methodology is described. Simulation results are given in Section 3 follows by section 4 that optimized antenna results are presented. Finally, summary and conclusions are provided in Section 5.

2. Antenna Configuration

A comprehensive design methodology for FSIW is as follows: First, an SIW is designed for the frequency range of 20-30 GHz. The cutoff frequency

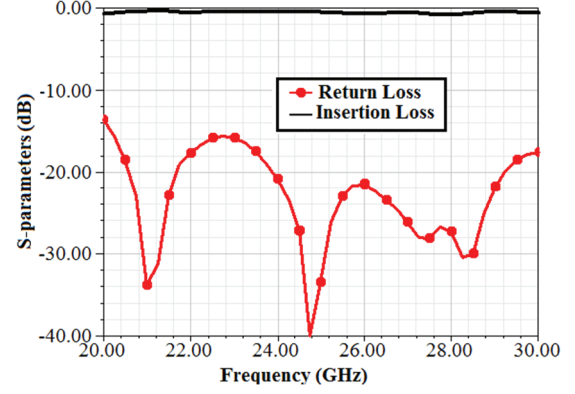


Fig. 2: Return loss and insertion loss of the FSIW to Strip line transition

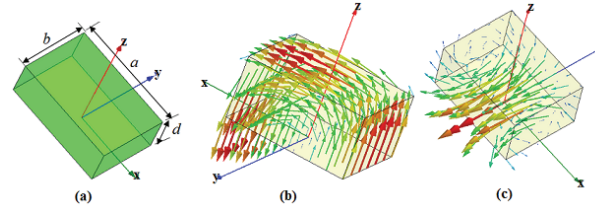


Fig. 3: (a) RDRA configuration (b) E field at 20GHz (c) H field at 20GHz

of the SIW must be 10GHz that is one decade lower than 20 GHz. Then from parameters of SIW the dimensions of the FSIW and its propagation constant are calculated based on [18]

$$a_{FSIW} = a_{SIW} - a/2$$

$$a = a_{SIW} + \frac{s}{2} \ln\left(\frac{s}{2d}\right) \quad (1)$$

$$g = \frac{ah}{2h + 1.3ae^t} + \frac{a' - a}{2} \quad (2)$$

$$t = \frac{(a')^2}{2ah} \cot\left(\frac{\pi a}{2a'}\right)$$

Where d is the via diameter, s is the distance between two neighbouring vias, h is each substrate height and other parameters are as shown in Figure 1.

Also, for design of an SIW [16]

$$a_{RWG} = a_{SIW} - 1.08 \frac{d^2}{s} + 0.1 \frac{d^2}{a_{SIW}} \quad (3)$$

Where a_{RWG} is the width of the equivalent rectangular waveguide with solid walls that is obtained based on the desired cutoff frequency which depends on our design operating band, then from this value and by considering that $s/d < 2$, $d/w < 1.5$, the SIW width, a_{SIW} , is obtained. The dielectric substrate is ROGERS 5880 with the dielectric constant of $\epsilon_r = 2.2$. Based on these equations the FSIW and SIW parameters are calculated to be:

$$d = 0.6mm \quad h = 0.508mm, \quad a_{RWG} = 10.11mm, \quad s/d = 1.5$$

$$d/w = 0.075, \quad s = 0.9mm, \quad a_{SIW} = 10.68mm,$$

$$a_{FSIW} = 5.41mm, \quad g = 0.37mm.$$

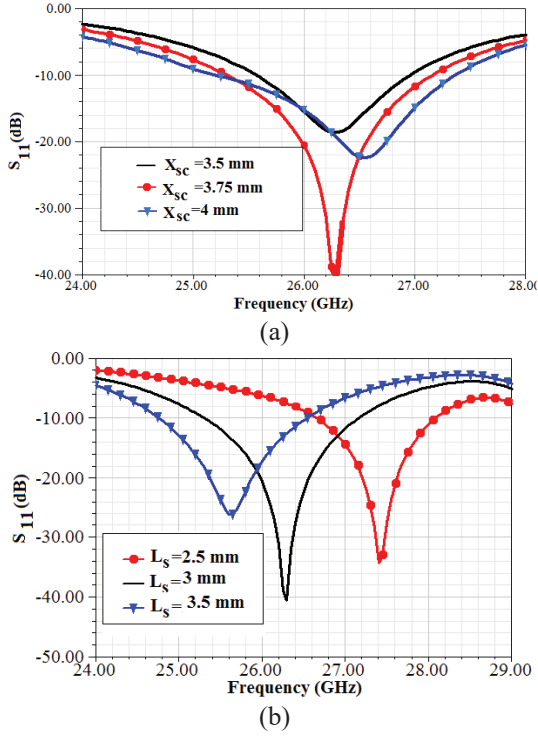


Fig. 4: Reflection coefficient for various values of (a) X_{SC} , $L_s = 3mm$, $W_s = 0.5mm$, $dd = 0mm$, $tt = 2.2mm$. (b) Slot length, L_s , $X_{SC} = 3.75mm$, $W_s = 0.5mm$, $dd = 0mm$, $tt = 2.2mm$.

Where as shown in Figure 1(b) g is the gap between the central metal layer and the right cylindrical side walls.

Also, Figure 1(b) depicts a transition from strip line to FSIW which is integrated on the same substrate of FSIW and strip line ones. The dimensions of the transition (i.e. p and q) must be optimized to minimize the insertion loss and improve the return loss. Figure 2 shows that for $p = 3mm$, $q = 1.5mm$ the return loss and insertion loss is improved.

Figure 3 depicts the rectangular dielectric resonator antenna (RDRA) that resonates in TE_{111}^y mode. The resonance frequency of this mode can be determined using the dielectric waveguide model [10]

$$f_0 = \frac{c}{2\pi\sqrt{\epsilon_r}} \sqrt{k_x^2 + k_y^2 + k_z^2} \quad (4)$$

$$k_x = \frac{\pi}{a}, k_z = \frac{\pi}{2d}$$

$$\tan\left(\frac{k_y b}{2}\right) = \frac{\sqrt{(\epsilon_r - 1)k_0^2 - k_y^2}}{k_y}$$

Where a , b and d are as depicted in Figure 3, c is the speed of light in the vacuum and $\epsilon_r = 10.2$ is the dielectric constant of the DR. The DR is made from ROGERS 6010. By solving this equation a , b , d are calculated to be: $a = 4.5mm$, $b = 2mm$, $d = 1.9mm$. In order to strongly excite TE_{111}^y mode, a source (slot) should be located at a strong field (magnetic) to ensure

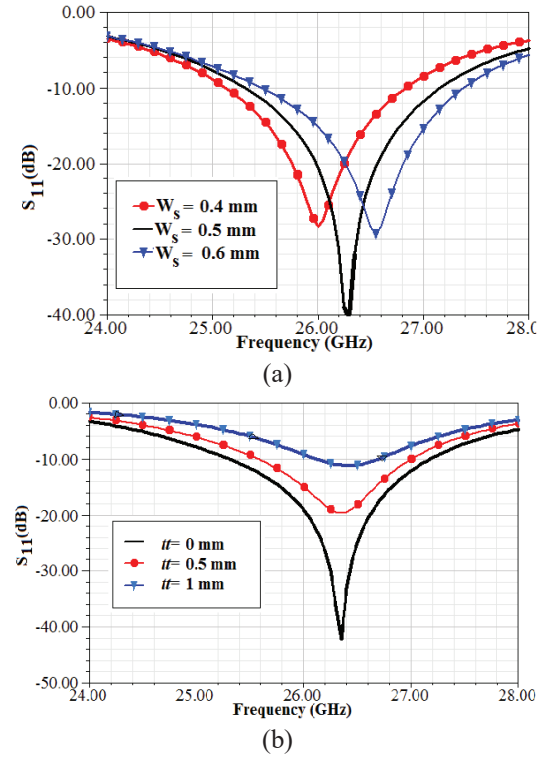


Fig. 5: Reflection coefficient for various values of (a) slot width, W_s , $X_{sc} = 3.75mm$, $L_s = 3mm$, $tt = 2.2mm$, $dd = 0mm$. (b) dd , $X_{sc} = 3.75mm$, $L_s = 3mm$, $W_s = 0.5mm$, $dd = 0mm$.

a good coupling. From Figure 3(c) observe that the slot aperture must be placed parallel to y axis beneath the DRA. So, in the next step the best place in the top metal layer of the FSIW for etching a slot aperture must be determined.

A comprehensive design methodology for FSIW is as follows: First, an SIW is designed for the frequency range of 20-30 GHz. The cutoff frequency of the SIW must be 10GHz that is one decade lower than 20 GHz. Then from parameters of SIW the dimensions of the FSIW and its propagation constant are calculated based on [18]

$$a_{FSIW} = a_{SIW} - a/2$$

$$a = a_{SIW} + \frac{s}{2} \ln\left(\frac{s}{2d}\right) \quad (1)$$

$$g = \frac{ah}{2h + 1.3ae^t} + \frac{a' - a}{2} \quad (2)$$

$$t = \frac{(a')^2}{2ah} \cot\left(\frac{\pi a}{2a'}\right)$$

Where d is the via diameter, s is the distance between two neighbouring vias, h is each substrate height and other parameters are as shown in Figure 1.

Also, for design of an SIW [16]

$$a_{RWG} = a_{SIW} - 1.08 \frac{d^2}{s} + 0.1 \frac{d^2}{a_{SIW}} \quad (3)$$

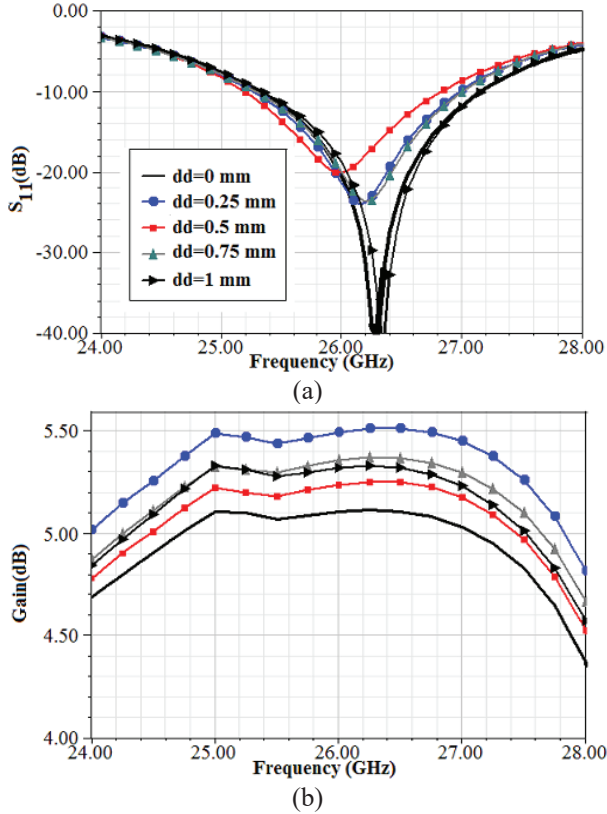


Fig. 6: (a) Reflection Coefficient and (b) Gain of the proposed antenna for different values of dd with other parameter values set as follows: $X_{sc} = 3.75\text{mm}$, $L_s = 3\text{mm}$, $W_s = 0.5\text{mm}$, $tt = 0\text{mm}$.

Table 1: Optimized Parameters of the FSIW-DRA Antenna

Parameter	value
X_{SC}	3.75 mm
L_S	3 mm
W_S	0.5 mm
dd	0 mm
tt	0.25 mm

Where a_{RWG} is the width of the equivalent rectangular waveguide with solid walls that is obtained based on the desired cutoff frequency which depends on our design operating band, then from this value and by considering that $s/d < 2$, $d/w < 1.5$, the SIW width, a_{SIW} , is obtained. The dielectric substrate is Rogers 5880 with the dielectric constant of $\epsilon_r = 2.2$.

Based on these equations the FSIW and SIW parameters are calculated to be: $d = 0.6\text{mm}$, $h = 0.508\text{mm}$, $a_{RWG} = 10.11\text{mm}$, $s/d = 1.5$, $d/w = 0.075$, $s = 0.9\text{mm}$, $a_{SIW} = 10.68\text{mm}$, $a_{FSIW} = 5.41\text{mm}$, $g = 0.37\text{mm}$. Where as shown in Figure 1(b) g is the gap between the central metal layer and the right cylindrical side walls. Also, Figure 1(b) depicts a transition from strip line to FSIW which is integrated on the same substrate of FSIW and strip line ones. The dimensions of the

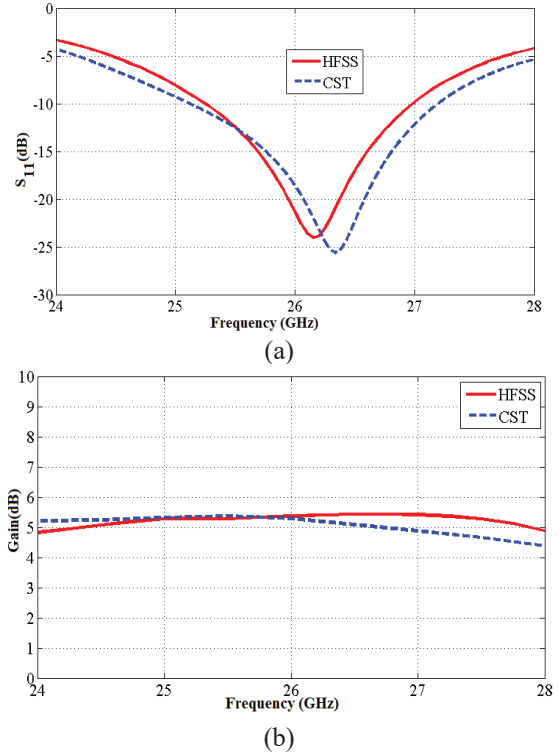


Fig. 7: The proposed antenna (a) reflection coefficient (b) gain from both simulation softwares, namely HFSS and CST, $X_{SC} = 3.75\text{mm}$, $L_s = 3\text{mm}$, $W_s = 0.5\text{mm}$, $tt = 0\text{mm}$, $dd = 0.25\text{mm}$.

transition (i.e. p and q) must be optimized to minimize the insertion loss and improve the return loss. Figure 2 shows that for $p = 3\text{mm}$, $q = 1.5\text{mm}$ the return loss and insertion loss is improved.

Figure 3 depicts the rectangular dielectric resonator antenna (RDRA) that resonates in TE_{111}^y mode. The resonance frequency of this mode can be determined using the dielectric waveguide model [10]

$$f_0 = \frac{c}{2\pi\sqrt{\epsilon_r}} \sqrt{k_x^2 + k_y^2 + k_z^2} \quad (4)$$

$$k_x = \frac{\pi}{a}, k_z = \frac{\pi}{2d}$$

$$\tan\left(\frac{k_y b}{2}\right) = \frac{\sqrt{(\epsilon_r - 1)k_0^2 - k_y^2}}{k_y}$$

Where a , b and d are as depicted in Figure 3, c is the speed of light in the vacuum and $\epsilon_r = 10.2$ is the dielectric constant of the DR. The DR is made from ROGERS 6010. By solving this equation a , b , d are calculated to be: $a = 4.5\text{mm}$, $b = 2\text{mm}$, $d = 1.9\text{mm}$. In order to strongly excite TE_{111}^y mode, a source (slot) should be located at a strong field (magnetic) to ensure a good coupling. From Figure 3(c) observe that the slot aperture must be placed parallel to y axis beneath the DRA. So, in the next step the best place in the top metal layer of the FSIW for etching a slot aperture must be determined.

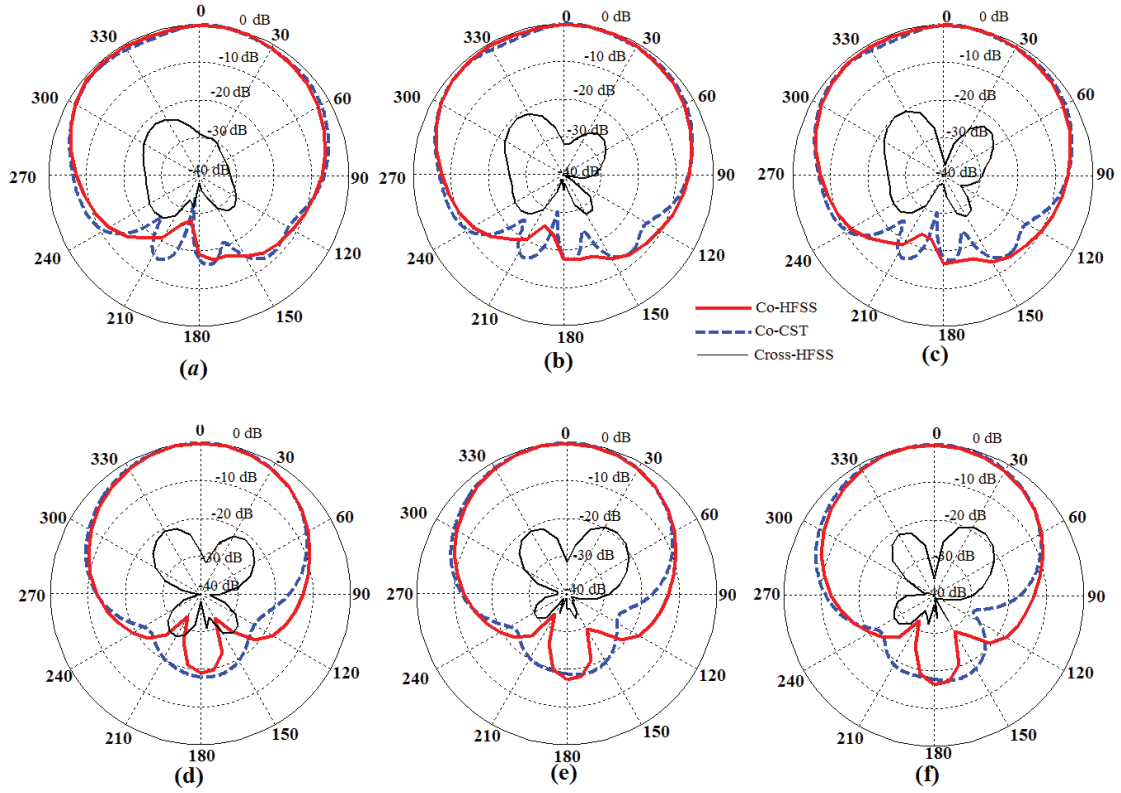


Fig. 8 The simulated radiation patterns of the proposed antenna for parameter values are listed in Table I in (a) E plane(XZ plane) at 25 GHz (b) E plane(XZ plane) at 26 GHz (c) E plane(XZ plane) at 27 GHz (d) H plane(YZ plane) at 25 GHz (e) H plane(YZ plane) at 26 GHz (f) H plane(YZ plane) at 27 GHz.

3. Simulation Results

Figure 1(c) depicts the RDRA fed by an FSIW. For designing the proposed antenna first, the initial values from design formulas are calculated then a comprehensive parametric study with the aid of electromagnetic simulation tool Ansoft HFSS is carried out to optimize the antenna parameters. Furthermore, in order to maximize energy coupling from the FSIW interior to the dielectric resonator, the slot is positioned at a distance of $X_{SC} = n\lambda_g / 2, n = 1, 2, 3, \dots$ from the FSIW shorting end which corresponds to a maximum intensity of magnetic field inside the FSIW. Additionally, in order to enhancing the slot-RDRA coupling other parameters such as slot length, slot width, RDRA-slot relative position, and position of the slot relative to the center of FSIW must be optimized. As the FSIW and DRA are designed, the FSIW guided wavelength (λ_g) is calculated according to Eq.4 where the phase constant k_z can be determined by [13, Eq (13)].

$$\lambda_g = 2\pi / k_z \quad (4)$$

So, the guided wavelength of the FSIW is calculated to be $\lambda_g = 11.52mm$. Nevertheless, the distance of slot center from the FSIW shorting end is determined to be $X_{SC} = 5.76mm$. Also, for a good excitation of the DRA the slot length should be changed in the vicinity of $\lambda/2$, where corresponds to natural resonance frequency of the slot.

3.1 Slot position relative to FSIW shorting end, X_{SC}

For attaining the best impedance matching, X_{SC} must be optimized. The magnetic field intensity along the y axis is maximum near the right sidewall. Hence, the slot is etched in this region on top metallic sheet of the FSIW and the DRA is placed in right side of the slot for initial state in the parametric study. Therefore, the parameter initial values are as follows: $tt = 2.2mm, dd = 0mm, X_{SC} = 5.76mm$.

The simulation curves of Figure 4(a) show how the reflection coefficient varies as the X_{SC} changes with other parameters fixed. Observe that for $X_{SC} = 3.75mm$ best impedance matching is achieved. This value is different from that obtained by theoretical calculations. Note that the guided wavelength at 25 GHz is 8.76 mm and the half of this value is 4.38 mm that is near to simulation ones.

3.2 Slot length, L_S

The variation of the reflection coefficient with the slot length L_S is illustrated in Figure 4(b). The simulation curves show that by increasing the slot length, the resonance frequency, i.e., minimum point position in curve, is shifted toward the lower frequencies. Best impedance matching is achieved for the slot length of 3 mm.

3.3 Slot width, W_S

Figure 5(a) depicts the impact of slot width variation on the reflection coefficient of the proposed antenna. By increasing the slot width, the resonance frequency is increased. Note that in order to avoid cross-polarized radiation the slot width is selected as $W_S < \lambda_0 / 20$, where λ_0 is the free space wavelength at 20GHz. As a

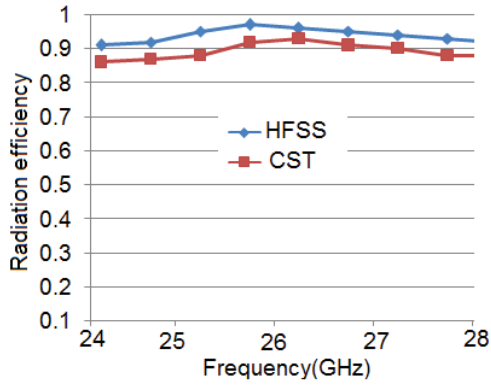


Fig. 6 The radiation efficiency of the proposed antenna from both simulators, HFSS and CST.

result, the value of $W_s = 0.5\text{mm}$ leads to best impedance matching.

3.4 Slot position relative to central metal layer edge, tt

From Figure 5(b) observe that whatever the slot and DRA are shifted away from the right sidewall of the FSIW, the coupling between the FSIW and DRA is weakened. This behavior is because of the magnetic field intensity where near the right sidewall is stronger. Hence, the initial positions of the slot and DRA are implied to be near the right sidewall.

3.5 DRA position relative to slot, dd

Figures 6(a), (b) depict the effect of dd variation on the reflection coefficient and gain of the DR-FSIW antenna which dd is distance between the DR and slot right sides. Observe that best gain is achieved for dd=0.25 mm. Furthermore, best impedance matching is achieved for dd=0mm and 1mm. But, since the impedance bandwidth for dd=0.25 mm is nearly same as that for 0,1 mm and beside its gain is considerably better, the value of dd is better to be 0.25 mm.

4 Optimized Antenna

Optimized parameters of the antenna depicted in Figure 1(c) are listed in Table I. Then, based on these values the antenna is simulated. Figure 7 shows the proposed antenna reflection coefficient and gain. It is observed that the impedance bandwidth of the antenna is 6.7% from 25.25 to 27 GHz and its gain has a good value above 5 dB over whole frequency bandwidth. Also, from Figure 7(a) it is observed that the DRA resonates at 26.5 GHz (frequency correspond to the minimum point in the reflection coefficient curve) that differs from the value obtained by theory, i.e., 20 GHz. This discrepancy is because of the slot etching in the ground plane. In fact, the theoretical formulation is based on the assumption of infinite ground plane without defect in beneath the DR. As a result, the slot in the ground plane shifts the resonance frequency to a higher frequency of 26.5 GHz. Figure 8 shows FSIW based RDRA radiation patterns in both E and H planes. As we can see at three sample frequencies from operating band, the radiation patterns are broadside type. Since the slot width is selected to minimize the

cross-polarization level, the simulated cross polarization levels are at least -16 dB below the main beam level. Also, Figure 9 depicts radiation efficiency of the DR-FSIW antenna. Observe that the proposed antenna has a good efficiency better than 87% in the frequency range of 25 to 27 GHz. This good efficiency was predictable because of good radiation efficiency of DRA and high Q factor of FSIW that prevent radiation loss.

4. Conclusions

In this paper, a novel low loss/profile aperture coupled DRA has been studied. The FSIW feeding have advantages of having half width of SIW, preventing parasitic radiations, having high Q factor and low losses in higher frequencies specially at millimeter wave region. The numerical simulated results show an impedance bandwidth of 6.7% from 25.25 GHz to 27 GHz and a good gain of about 5 dB together with a relatively high radiation efficiency at least 0.87 over this range.

Reference

- [1] S.A.Long, M. McAllister, and L.C. Shen, "The resonant cylindrical cavity antenna," *IEEE Transactions on Antennas and Propagation*, vol. 31, pp. 406-412, May 1983.
- [2] A. Petosa, *Dielectric Resonator Antenna Handbook*, Norwood, MA, Artech House, 2007.
- [3] W. M. Abdel Wahab, D. Busuioc, and S. Safavi-Naeini, "Low cost planar waveguide technology-based dielectric resonator antenna (DRA) for millimeter-wave applications: Analysis, design, and fabrication," *IEEE Transactions on Antennas and Propagation*, vol. 58, no. 8, pp. 2499-2507, Aug 2010.
- [4] S. Fakhte, H. Oraizi and R. Karimian, "A Novel Low-Cost Circularly Polarized Rotated Stacked Dielectric Resonator Antenna," in *IEEE Antennas and Wireless Propagation Letters*, vol. 13, no. , pp. 722-725, 2014.
- [5] Chih-Yu Huang, Jian-Yi Wu, and Kin-Lu Wong, "Cross-slot-coupled microstrip antenna and dielectric resonator antenna for circular polarization," *IEEE Transactions on Antennas and Propagation*, vol. 47, no. 4, pp. 605-609, April 1999.
- [6] Q. Rao, T. A. Denidni, and A. R. Sebak, "Broadband compact stacked T-shaped dra with equilateral-triangle cross sections," *IEEE Microwave and Wireless Components Letters*, vol. 16, no. 1, pp. 7-9, Jan 2006.
- [7] M. Abedian, S. K. A. Rahim, and M. Khalily, "Two-segments compact dielectric resonator antenna for UWB application," *IEEE Antennas*

- and *Wireless Propagation Letters*, vol. 11, pp. 1533–1536, 2012.
- [8] E. Baldazzi *et al.*, "A High-Gain Dielectric Resonator Antenna With Plastic-Based Conical Horn for Millimeter-Wave Applications," in *IEEE Antennas and Wireless Propagation Letters*, vol. 19, no. 6, pp. 949-953, June 2020.
- [9] A. Petosa and S. Thirakoune, "Rectangular dielectric resonator antennas with enhanced gain," *IEEE Transactions on Antennas and Propagation*, vol. 59, no. 4, pp. 1385–1389, Apr. 2011.
- [10] K.W. Luk and K.W. Leung, eds. *Dielectric Resonator Antennas*, Hertfordshire, England, Research Studies Press, 60-61, 2003.
- [11] K. Moradi, and S. Nikmehr, "A dual-band dual-polarized Microstrip array antenna for base stations," *Progress In Electromagnetics Research*, Vol. 123, 527-541, 2012.
- [12] Xu, H.-Y., H. Zhang, K. Lu, and X.-F. Zeng, "A holly-leaf-shaped monopole antenna with low RCS for UWB application," *Progress In Electromagnetics Research*, Vol. 117, 35-50, 2011.
- [13] A. Petosa, *Dielectric Resonator Antenna Handbook*, ArtechHouse, 2007, Norwood, MA.
- [14] Petosa, A., A. Ittipiboon, Y. M. M. Antar, and D. Roscoe, "Recent advances in dielectric resonator antenna technology," *IEEE Antennas and Propagation Magazine*, Vol. 40, No. 3, 35–48, June 1998.
- [15] W. M. Abdel Wahab, D. Busuioc, and S. Safavi-Naeini, "Modeling and design of millimeter-wave high Q-factor parallel feeding scheme for dielectric resonator antenna arrays," *IEEE Antenna and wireless propagation letters*, Vol. 10, 2011.
- [16] X. Feng and W. Ke, "Guided-wave and leakage characteristics of substrate integrated waveguide," *IEEE Trans. Microw. Theory Tech.*, vol. 53, no. 1, pp. 66–73, Jan. 2005.
- [17] Q. H. Lai, C. Fumeaux, W. Hong, and R. Vahldieck, "Characterization of the propagation properties of the half-mode substrate integrated waveguide," *IEEE Trans. Microw. Theory Tech.*, vol. 57, no. 8, pp.1996–2004, Aug. 2009.
- [18] Wenquan Che, Liang Geng, Kuan Deng, and Y. Leonard Chow, "Analysis and experiments of compact folded substrate integrated waveguide," *IEEE Trans. Microw. Theory Tech.*, vol. 56, no. 1, pp.88-93, Jan.2008.